

Wolfenstein parameters for $s_{1/2}$ proton knockout ($p, 2p$) reactions

T. Noro,^{1,*} M. Kawabata,^{2,†} G. C. Hillhouse,³ S. Akimune,⁴ H. Akiyoshi,^{1,‡} I. Daito,^{2,§} K. Hatanaka,² M. Itoh,^{5,||} Y. Maeda,² N. Matsuoka,² S. Morinobu,² M. Nakamura,^{5,¶} A. Okihana,⁶ H. Sagara,¹ H. Sakaguchi,^{5,**} K. Takahisa,² H. Takeda,⁷ A. Tamii,² K. Tamura,^{2,††} H. Toyokawa,⁸ H. Yamazaki,⁹ H. P. Yoshida,^{2,||} and M. Yosoi²

¹Department of Physics, Kyushu University, Fukuoka 812-8581, Japan

²Research Center for Nuclear Physics, Osaka University, Ibaraki, Osaka 567-0047, Japan

³Department of Physics, University of Stellenbosch, Stellenbosch 7600, South Africa

⁴Department of Physics, Konan University, Kobe 658-8501, Japan

⁵Department of Physics, Kyoto University, Kyoto 606-8502, Japan

⁶Kyoto University of Education, Kyoto 612-8522, Japan

⁷Institute of Physical and Chemical Research (RIKEN), Wako 351-0198, Japan

⁸Japan Synchrotron Radiation Research Institute, Hyogo 679-5198, Japan

⁹Laboratory of Nuclear Science, Tohoku University, Sendai 982-0826, Japan

(Received 31 December 2007; published 23 April 2008)

A complete set of Wolfenstein parameters ($D_{i'j}$), induced polarizations (P), and analyzing powers (A_y) have been measured for ($p, 2p$) reactions on ${}^6\text{Li}$, ${}^{12}\text{C}$, and ${}^{40}\text{Ca}$ targets in order to investigate possible nuclear medium effects on the nucleon-nucleon (NN) interaction. Most of these observables show significant reductions from the values for proton-proton scattering as monotonic functions of the nuclear density relevant to these reactions. The reductions of these $D_{i'j}$ are reasonably reproduced by nonrelativistic plane-wave and distorted-wave calculations based on the impulse approximation, demonstrating that these suppressions are attributed to changes of the two body kinematics due to the finite separation energies of these reactions, while the reductions of A_y and P are much more prominent than the calculations. The relativistic calculations, which partly explain the A_y and P reductions, cannot reproduce the $D_{i'j}$ data, but all the data are consistently reproduced when the parameters of the NN interaction in a meson exchange model are renormalized, suggesting possible modifications of the NN interaction by the surrounding nuclear medium.

DOI: [10.1103/PhysRevC.77.044604](https://doi.org/10.1103/PhysRevC.77.044604)

PACS number(s): 21.30.-x, 24.10.-i, 24.70.+s, 25.40.-h

I. INTRODUCTION

Exclusive measurements of nucleon knockout reactions by nucleons, e.g., ($p, 2p$) reactions, give a direct means to study the effect of the nuclear field on the nucleon-nucleon (NN) interaction due to Pauli blocking and Fermi motion. In addition to these effects, nontrivial nuclear medium effects at the hadron level are theoretically predicted. An enhancement of the lower components of Dirac spinors is predicted in the framework of quantum hadrodynamics (QHD) [1,2] and reductions of hadron masses are predicted in the context of QCD [3–13]. Since the NN interaction is well described by theoretical models based on meson exchange forces, it is

natural to consider that such modifications of hadron properties also influence the NN interaction [14]. At incident nucleon energies of several hundred MeV, the reaction mechanism of nucleon knockout reactions is expected to be relatively simple [15,16]. In addition, a significant contribution from the nuclear interior, where the nuclear density is considerably high, is expected in these reactions [17]. Therefore, knockout reactions should be ideal probes for investigating the NN interaction in the nuclear medium, which in turn may reflect on medium effects at the hadron level.

In several experiments it has been observed that the analyzing power (A_y) for quasifree proton scattering is significantly suppressed from values which are given by theoretical predictions based on the NN interaction in free space. The suppression of A_y in ($p, 2p$) reactions was first observed at TRIUMF for proton knockout from the $1s_{1/2}$ orbit of ${}^{16}\text{O}$ target at an incident energy of 500 MeV [18,19]. This work was extended to $1s_{1/2}$ knockout from many target nuclei at RCNP at an incident energy of 392 MeV [17,20]. The results show that the A_y values are systematically suppressed as a monotonic function of either the separation energies or the effective mean densities, except for very light target nuclei such as He isotopes. At PNPI, in addition, a similar kind of suppression has been observed for the induced polarization (P) at an incident energy of 1 GeV and for a wide range of outgoing proton energies [21,22]. The latter experimental evidence strongly suggests that these suppressions are not caused by contamination from multi-step processes, but rather are

*norono@phys.kyushu-u.ac.jp

†Deceased.

‡Present address: Institute of Physical and Chemical Research (RIKEN), Wako 351-0198, Japan.

§Present address: Kansai Photon Science Institute, Japan Atomic Energy Agency, Kizugawa, Kyoto 619-0215, Japan.

||Present address: Cyclotron and Radioisotope Center, Tohoku University, Sendai 980-8578, Japan.

¶Present address: Wakayama Medical University, Wakayama 641-8509, Japan.

**Present address: Faculty of Engineering, Miyazaki University, Miyazaki 889-2192, Japan.

††Present address: Faculty of Medical Sciences, University of Fukui, Fukui 910-1193, Japan.

attributed to some nuclear medium effect, since the effective mean densities amount to about one-third of the saturation density in the highest case.

At present, there are no theoretical models which describe these suppressions quantitatively. The TRIUMF data were compared to a number of theoretical predictions, namely the nonrelativistic distorted wave impulse approximation (DWIA) with empirical density-dependent modifications and relativistic effective-mass corrections, as well as predictions based on the full relativistic DWIA. A conclusion of these works were that all of these calculations failed to reproduce the A_y [19,23]. The RCNP data were also compared to similar types of calculations [20,24,25]. One of the important points shown by these comparisons is that the suppression of A_y is clearly observed even for kinematical conditions where the recoil momentum of the residual nucleus is zero. Calculations show that nonrelativistic distortion effects to A_y are exceptionally small for those kinematics and, therefore, the A_y suppressions are not attributed to nuclear diffraction and absorption effects. In addition, suppressions are consistently observed for a wide energy range. These results support the idea that the spin dependence of the NN scattering amplitude is modified in the nuclear field. For further investigation of this view point, experimental data on polarization transfer coefficients are expected to give new tests for theoretical models.

Polarization transfer coefficients (Wolfenstein parameters D_{ij}) in nucleon quasifree scattering have been extensively studied only for inclusive (p, p') and (p, n) reactions. These data were measured at LAMPF and at RCNP in order to examine the possible enhancement of the spin longitudinal responses caused by pion correlations in the nuclear field [26–30]. Against the theoretical predictions, however, clear enhancements were not observed and the ratios of spin longitudinal and transverse responses were close to values theoretically predicted without correlations. In addition, the LAMPF (p, p') data have been compared with a prediction based on the relativistic PWIA [31] and it was shown that almost all of the polarization transfer data, except A_y and P , were close to a prediction with a free nucleon mass in the Dirac spinors, which is equivalent to nonrelativistic predictions with NN interactions in free space. A measurement of complete sets of polarization transfer observables for the inclusive reaction was also performed at TRIUMF [32]. Comparison of the latter with a DWIA calculation again showed that the polarization transfer coefficients are reasonably predicted by a Fermi gas model with free NN interactions in contrast to the A_y case. For polarization transfer coefficients in exclusive proton quasifree scattering, only a limited number of spin observables, namely $D_{s'l}$ and $D_{s's}$, have been measured [19]. The $D_{s's}$ data show a meaningful deviation from the DWIA prediction, but due to ambiguities caused by distortion effects this is not clear enough for these data, since a wide energy region is integrated to obtain the data. Recently, polarization transfer coefficients for ${}^4\text{He}(\vec{e}, e'\vec{p})$ were measured at Mainz [33] and Jefferson Lab [34] in order to investigate medium modifications of the proton form factors. The result favors the inclusion of a medium effect predicted by a quark-meson coupling model, though it is not conclusive enough.

In this article, we present our measurements of polarization transfer coefficients, D_{nn} , $D_{s's}$, $D_{l'l}$, $D_{s'l}$, and $D_{l's}$, as well as A_y and P , for $(p, 2p)$ reactions. These are the first data of polarization transfer coefficients for the zero-recoil kinematical condition being employed. In particular, these are first data of a complete set of the Wolfenstein parameters for this reaction. It is well known that different spin observables are sensitive to different model ingredients and hence, complete sets of polarization transfer observables provide extremely stringent tests for theoretical models. In this paper we exploit this discriminatory nature in order to identify observables which allow one to extract information regarding the role of the nuclear medium in modifying the NN interaction relative to its value in free space.

As described above, the A_y suppression at 392 MeV and higher energies has not been quantitatively explained by any theoretical models. However, at 202 MeV, the dynamical relativistic model has succeeded in reproducing the A_y data for ${}^{208}\text{Pb}(p, 2p)$ reaction, which is significantly reduced compared to nonrelativistic predictions [35,36]. Indeed, this relativistic model consistently accounts for about half of the reduction at both of 392 MeV and 1 GeV [25], while nonrelativistic medium effects completely fail to reproduce this phenomenon [24]. In addition, Krein *et al.* have demonstrated that the inclusion of medium-modified meson masses and coupling constants via a relativistic one boson exchange model cause a drastic reduction of A_y [37]. In this paper, therefore, the experimental data are compared with theoretical calculations based on both of the nonrelativistic and relativistic models and we examine the sensitivities of the spin observables to various model ingredients, especially those related to the relativistic treatment.

The experimental detail is described in the next section, and the relevant theoretical models are described in Sec. III. In Sec. IV we compare model predictions to our data, and we summarize and conclude in Sec. V.

II. EXPERIMENTAL DETAILS

A. Polarized proton beams

The exclusive $(p, 2p)$ experiment was performed using the cyclotron complex at RCNP, Osaka. The energy of the beam, 392.2 ± 1.4 MeV, was determined [38] from the momentum ratio of elastically and inelastically scattered protons from a carbon target, which was precisely measured using the high resolution spectrometer, Grand Raiden [39].

In order to measure a complete set of Wolfenstein parameters, polarized proton beams with three different polarization directions are required. Polarized protons were produced in an atomic beam polarized ion source [40] and were first accelerated by the injector AVF cyclotron. The polarization axis of the beam in this cyclotron was normal to the accelerating plane. The beam was re-accelerated by the main ring cyclotron and transported as a vertically polarized beam to the target chamber for spectrometer experiments. Two kinds of horizontally polarized beams were prepared by activating either of two solenoid magnets in the injection beam line to the ring cyclotron. The proton spins were rotated from the vertical

direction to the horizontal direction which was perpendicular to the beam line at the magnet. The bending angle of the beam line between these solenoid magnets was 45° , which corresponds to a spin precession angle of 86.2° relative to the beam direction at the injection energy of 64.2 MeV. The polarization direction of these beams were not necessarily parallel nor perpendicular to the beam direction at the target position, but the relative angle was almost conserved even after acceleration by the ring cyclotron.

All three components of the beam polarization were monitored using two sets of beam-line polarimeters (BLP) in the WN-beam line between the ring cyclotron and the target chamber. The bending angle of the beam line between these BLPs was 50° and proton spins precess by 127.1° , again relative to the beam direction, due to this bending. The beam line had no bending elements between the downstream BLP and the target chamber. At each polarimeter, proton-proton scattering using a polyethylene target was observed employing a coincidence method. The detection angle of the forward outgoing protons was 17° and the effective analyzing power was 0.45 ± 0.01 . The actual beam polarization ranged between 0.65 and 0.75.

B. Spectrometer system

Two outgoing protons from CH_2 , ${}^6\text{Li}$ (and ${}^6\text{LiO}$ for contamination subtraction), ${}^{\text{nat}}\text{C}$, and ${}^{\text{nat}}\text{Ca}$ target foils were momentum analyzed in coincidence using the two-arm spectrometer system, consisting of the Grand Raiden (GR) spectrometer [39] and the Large Acceptance Spectrometer (LAS) [41]. A schematic view of the system is given in Fig. 1. The setting angles and the central energies of the spectrometers correspond to the kinematic condition where the recoil momentum is zero for each target with different separation energies for the $s_{1/2}$ orbits. In a plane wave limit, this condition corresponds to knockout of bound protons with zero Fermi momentum. These settings are similar to those employed in Ref. [20], but slightly different from those in Ref. [17], where angle settings of both spectrometers and the energy settings of forward outgoing protons were the same as those for free p - p scattering. The actual recoil momenta range up to $25 \text{ MeV}/c$ in

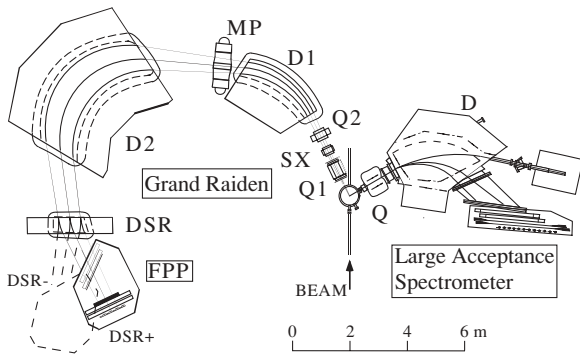


FIG. 1. The two-arm spectrometer system at RCNP: D, D1, and D2 denote dipole magnets, Q, Q1, and Q2 quadrupole magnets, SX a sextupole magnet, while MP is a multipole magnet for aberration correction. See the text for polarization transfer measurements using the DSR and the FPP.

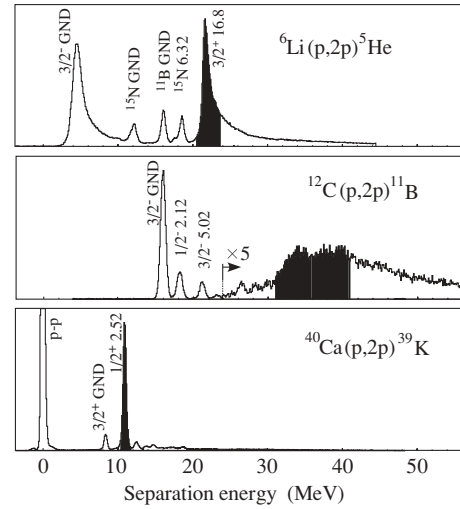


FIG. 2. Separation energy spectra for $(p, 2p)$ reactions. Each vertical axis is a linear scale in arbitrary units. The shaded areas are used for determining the $D_{l'j}$ values. In the case of the ${}^6\text{Li}$ target, the contribution from ${}^{12}\text{C}$ and ${}^{16}\text{O}$ contaminations, included in the shaded regions, are subtracted by using experimental data for ${}^6\text{LiO}$ and ${}^{\text{nat}}\text{C}$ targets.

the standard deviation because of finite acceptance angles and finite momentum bites. The solid angles were 4.3 msr and 20 msr, which were the maximum acceptances and corresponded to $\pm 20 \text{ mr}$ and $\pm 50 \text{ mr}$ in the horizontal angle widths, for the GR and the LAS, respectively. The momentum bite of the GR was limited to $\pm 2.2\%$ of the central momentum, while that for the LAS was large enough to accept all of the corresponding protons.

At the focal plane of each spectrometer, two sets of vertical drift chambers (VDC's) were used and the positions and incident angles, in both of horizontal and vertical directions, of the detected protons were reconstructed. Using this information, the proton separation energies were calculated. Figure 2 shows separation-energy spectra for the three targets of interest. The overall energy resolution of the system is 350 keV FWHM for the ${}^{40}\text{Ca}(p, 2p)$ measurement. For this target, an adjacent peak of $7/2^-$ is not separated from the $1/2^+$ peak, but a nonrelativistic DWIA calculation estimates that the yield leading to this state is negligible.

C. Focal plane polarimeter and polarization transfer measurement

The polarization of protons at the focal plane of GR was measured using a focal plane polarimeter system (FPP) [42] following the VDC's. When incident protons for a nuclear reaction are polarized, the polarization vector of outgoing protons is described by

$$\begin{pmatrix} P_{s'} \\ P_{n'} \\ P_{l'} \end{pmatrix} = \frac{1}{1 + A_y P_n} \left[\begin{pmatrix} 0 \\ P \\ 0 \end{pmatrix} + \begin{pmatrix} D_{s's} & 0 & D_{s'l} \\ 0 & D_{n'n} & 0 \\ D_{l's} & 0 & D_{l'l} \end{pmatrix} \begin{pmatrix} P_s \\ P_n \\ P_l \end{pmatrix} \right], \quad (1)$$

where P_s ($P_{s'}$), P_n ($P_{n'}$), and P_l ($P_{l'}$) are the three components of the polarization vector in the incident (final) channel, A_y is the analyzing power, P is the induced polarization, and D_{ij} ($i, j = s, n, l$) represents the Wolfenstein parameters or the polarization transfer coefficients. This paper deals with $(p, 2p)$ reactions where two protons are ejected. We treat the forward ejected protons as the outgoing protons in the above equation and we adopt the Madison convention [43] for defining the coordinate system, namely, the directions of l and l' are taken to be in the same directions as the momenta of the incident proton \vec{p}_a and that of the forward outgoing proton \vec{p}_c , respectively, both the n - and n' -directions are the same as $\vec{p}_a \times \vec{p}_c$, and the third directions are taken so that (s, n, l) and (s', n', l') form a right handed coordinate system. Since the vertical direction is the same for both incoming and outgoing channels, including the coordinate system downstream from the spectrometers, we omit the prime “'” for the n direction hereafter.

The polarization vector of the outgoing protons is precessed by the dipole field of the GR and only the two components of the vector perpendicular to the momentum vector of protons at the FPP are actually measurable. For complete measurements of all three components, a dipole magnet for spin rotation (DSR) was prepared for Grand Raiden. This magnet is a bending magnet of either $+18^\circ$ or -17° , and the total bending angle of the central rays for the GR including the DSR is either $\alpha^{(+)} = 180.0^\circ$ or $\alpha^{(-)} = 145^\circ$. The spin precession angles caused by these bendings are given by the expression

$$\chi^{(\pm)} = \gamma \left(\frac{g}{2} - 1 \right) \alpha^{(\pm)}, \quad (2)$$

where g is the proton g -factor and γ is a Lorentz factor defined by $\gamma = (M_p c^2 + T_p) / M_p c^2$. Owing to these precessions, the polarization vectors of the outgoing protons are rotated and become

$$\begin{pmatrix} P_{s''}^{(\pm)} \\ P_n^{(\pm)} \\ P_{l''}^{(\pm)} \end{pmatrix} = \begin{pmatrix} \cos \chi^{(\pm)} & 0 & \sin \chi^{(\pm)} \\ 0 & 1 & 0 \\ -\sin \chi^{(\pm)} & 0 & \cos \chi^{(\pm)} \end{pmatrix} \begin{pmatrix} P_{s'} \\ P_n \\ P_{l'} \end{pmatrix} \quad (3)$$

at the FPP. From measurements of $P_n^{(+)}$ or $P_n^{(-)}$ using a vertically polarized beam, consisting of spin-up and spin-down modes, values for A_y , P and D_{nn} were deduced and, from measurements of $P_{s''}^{(+)}$ and $P_{s''}^{(-)}$ using the above mentioned two horizontally polarized beams, all of the other Wolfenstein parameters were determined.

The FPP consists of a 4–12 cm thick carbon-slab analyzer, two sets of multiwire proportional chambers (MWPC's), and two layers of scintillator hodoscopes. The polarization is calculated from left-right or up-down asymmetry of proton scattering from the carbon-slab employing raytracing with the MWPC's. Trigger signals for the data taking were coincidence signals of these hodoscopes and a scintillation counter located just downstream from the VDC's. Small-angle scattering events from the carbon analyzer were rejected by a fast second-level trigger system using position information from the MWPC's in order to reduce the trigger rate. The sizes of the MWPC's and the hodoscopes were large enough to cover the scattering angle θ_c up to 20° and all azimuthal angle ϕ_c of

the p -C scattering for the momentum bite of the GR mentioned above.

The effective analyzing power of the FPP is given by

$$A_y^{\text{eff}} = \frac{\int \sigma^{\text{inc}}(\theta_c) A_y^{\text{inc}}(\theta_c) \cos \phi_c d\Omega_c}{\int \sigma^{\text{inc}}(\theta_c) d\Omega_c}, \quad (4)$$

where $\sigma^{\text{inc}}(\theta_c)$ and $A_y^{\text{inc}}(\theta_c)$ refer to the cross section and the analyzing power for inclusive p -C scattering, respectively. Angular integration was performed over polar angles of $8^\circ \leq \theta_c \leq 20^\circ$ and azimuthal angles of $|\phi_c| \leq 60^\circ$ for the measurements of the vertical polarization, and $6^\circ \leq \theta_c \leq 20^\circ$ and the same ϕ_c region for measurements of the horizontal polarizations. The difference between the θ_c regions for these two kinds of measurements is caused by different settings of the second-level triggering. The A_y^{inc} was measured for this experiment in a wide incident energy region from 130 MeV to 392 MeV and it was confirmed that the result was consistent with an empirical formula proposed by a TRIUMF group [44]. The latter formula was actually employed for the present data analysis. Numerical values of the experimental data are summarized in Table I.

III. THEORETICAL MODELS

The experimental data are compared to theoretical calculations based on the relativistic and nonrelativistic DWIA, respectively. In all the cases, we adopt a zero range approximation for the two-body interactions. Since the formalisms for the relativistic and nonrelativistic distorted wave models have been presented in Refs. [25,35,36,45–47] and Refs. [25,48], respectively, we only briefly allude to the most important aspects of each model in this section.

A. Relativistic model

Let us consider a quasifree knockout reaction $A(a, cd)B$, where $A = b + B$. The relativistic transition matrix element in a zero-range approximation is given by

$$\begin{aligned} & T_{\text{LJM}_i}(s_a, s_c, s_d) \\ &= \int d\vec{r} [\bar{\Psi}_c^{(-)}(\vec{r}, \vec{k}_{cB}, s_c) \otimes \bar{\Psi}_d^{(-)}(\vec{r}, \vec{k}_{dB}, s_d)] \\ & \quad \times \hat{F}_{NN}(T_{\text{eff}}^{\text{lab}}, \theta_{\text{eff}}^{\text{c.m.}}) [\Psi_a^{(+)}(\vec{r}, \vec{k}_{aA}, s_a) \otimes \Phi_{\text{LJM}_j}(\vec{r})], \end{aligned} \quad (5)$$

where \otimes denotes the Kronecker product, $\Psi_i(\vec{r}, \vec{k}_{iB}, s_i)$ is the four-component distorted wave function of the particle i ($= a, c, d$) with momentum \vec{k}_{iB} and spin projection s_i , $\Phi_{\text{LJM}_j}(\vec{r})$ is the four-component bound-state wave function of particle b , and $\hat{F}_{NN}(T_{\text{eff}}^{\text{lab}}, \theta_{\text{eff}}^{\text{c.m.}})$ is the NN scattering matrix element which depends on the effective two-body kinetic energy $T_{\text{eff}}^{\text{lab}}$ and scattering angle $\theta_{\text{eff}}^{\text{c.m.}}$, taken with the so-called final energy description [49]. Note that the recoil corrections to the relativistic DWIA are excluded in this article, even though they are expected to play a significant role for light target nuclei such as ${}^6\text{Li}$ and ${}^{12}\text{C}$ [23].

The relativistic bound-state wave function $\Phi_{\text{LJM}_j}(\vec{r})$ is obtained via a self-consistent solution to the Dirac-Hartree field equations, of the relativistic mean field approximation,

TABLE I. Experimental polarization transfer coefficients, D_{ij} , analyzing powers, A_y , and induced polarizations, P , for exclusive proton knockout from the $1s_{1/2}$ states in ${}^6\text{Li}$ and ${}^{12}\text{C}$ as well as the $2s_{1/2}$ state in ${}^{40}\text{Ca}$ for an incident laboratory kinetic energy of 392 MeV and for kinematics corresponding to zero recoil momentum. Experimental data of p - p scattering corresponding to the same detection angle of 25.5° for forward outgoing protons are also given.

Target (orbit)	p - p	${}^6\text{Li}(1s_{1/2})$	${}^{12}\text{C}(1s_{1/2})$	${}^{40}\text{Ca}(2s_{1/2})$
θ_c	25.5°	25.5°	25.5°	25.5°
θ_d	-60.0°	-54.3°	-51.6°	-58.1°
T_c	307.4 MeV	281.0 MeV	268.0 MeV	298.0 MeV
T_d	84.6 MeV	86.5 MeV	88.0 MeV	85.7 MeV
P	0.336 ± 0.022	0.245 ± 0.019	0.191 ± 0.030	0.364 ± 0.021
A_y	0.359 ± 0.009	0.217 ± 0.008	0.127 ± 0.009	0.335 ± 0.011
D_{nn}	0.593 ± 0.028	0.526 ± 0.028	0.527 ± 0.042	0.561 ± 0.033
$D_{s's}$	0.403 ± 0.028	0.375 ± 0.041	0.343 ± 0.036	0.331 ± 0.034
$D_{s'l}$	0.214 ± 0.021	0.173 ± 0.046	0.150 ± 0.037	0.172 ± 0.031
$D_{t's}$	-0.284 ± 0.031	-0.199 ± 0.047	-0.175 ± 0.035	-0.319 ± 0.033
$D_{t'l}$	0.260 ± 0.020	0.227 ± 0.042	0.098 ± 0.038	0.207 ± 0.032

using the computer code TIMORA [50]. The distorted wave functions $\Psi_i(\vec{r}, \vec{k}_{iB}, s_i)$ are extracted by solving the Dirac scattering equation with spherical scalar and time-like vector proton-nucleus optical potentials. A global Dirac optical potential parameter set, compiled by the Ohio group [51] is used in calculations for ${}^{12}\text{C}$ and ${}^{40}\text{Ca}$ targets. On the other hand, we employed microscopic optical potentials based on the relativistic impulse approximation [50], which is consistent with the relativistic bound state wave function mentioned above, for the ${}^6\text{Li}$ calculations, since the global potential parameter set is not applicable for such a light nucleus.

For the NN scattering matrix linking the initial and final channels in the transition matrix element, we adopt the impulse approximation which assumes that the form of the NN scattering matrix in the nuclear medium is the same as that for free NN scattering. In particular, we employ the so-called IA1 representation, which parametrizes the five on-shell NN scattering amplitudes in terms of scalar, pseudoscalar, vector, axial-vector, and tensor invariants. In this representation, the parameters are determined from experimental NN scattering data. In particular, we utilize the SP07 phase-shift solution [52] for extracting the experimental p - p scattering amplitudes.

One of the aims of this paper is to study the sensitivity of complete sets of polarization transfer coefficients to density-dependent corrections to the NN matrix. For this purpose, we employ the Rho-Brown scaling conjecture [7] as applied by Krein *et al.* [37] to study nuclear medium effects in (p , $2p$) reactions, namely,

$$\frac{m_\sigma^*}{m_\sigma} = \frac{m_\rho^*}{m_\rho} = \frac{m_\omega^*}{m_\omega} \equiv \xi, \quad (6)$$

$$\frac{g_{\sigma N}^*}{g_{\sigma N}} = \frac{g_{\omega N}^*}{g_{\omega N}} \equiv \chi, \quad (7)$$

where the medium-modified and free meson masses are denoted by m_i^* and m_i , with $i \in (\sigma, \rho, \omega)$, respectively. Meson-nucleon coupling constants, with and without nuclear medium

modifications, are denoted by g_{jN}^* and g_{jN} , where $j \in (\sigma, \omega)$, respectively: see Sec. IV for typical values of ξ and χ .

For implementing the above conjecture, we adopt the relativistic Horowitz-Love-Franey (HLF) meson exchange model [53], whereby the direct and exchange contributions to the NN scattering amplitudes are parameterized separately in terms of a number of Yukawa-type meson exchanges in the first-order Born approximation. In this paper we employ Maxwell's parametrization (with energy-independent form factors) of the HLF amplitudes between 200 and 500 MeV [54]. Note that for relativistic predictions excluding density-dependent corrections to the NN interaction, we employ the experimental SP07 p - p scattering amplitudes as described above.

B. Nonrelativistic model

In the nonrelativistic framework based on the dynamical Schrödinger equation, the zero-range transition matrix element is given by

$$\begin{aligned} T_{\text{LJM}_j}^{\text{NR}}(s_a, s_c, s_d) &= \int d\vec{r} [\psi_c^{*(-)}(\vec{r}, \vec{k}_{cB}, s_c) \otimes \psi_d^{*(-)}(\vec{r}, \vec{k}_{dB}, s_d)] \hat{t}_{NN} \\ &\quad \times (T_{\text{eff}}^{\text{lab}}, \theta_{\text{eff}}^{\text{c.m.}}) [\psi_a^{(+)}(\gamma\vec{r}, \vec{k}_{aA}, s_a) \otimes \varphi_{\text{LJM}_j}(\vec{r})], \quad (8) \end{aligned}$$

where $\psi_i(\vec{r}, \vec{k}_{iB}, s_i)$ is the two-component scattering wave function of the incident ($i = a$) or outgoing ($i = c, d$) proton, $\varphi_{\text{LJM}_j}(\vec{r})$ is the wave function of the bound proton to be knocked out, $\hat{t}_{NN}(T_{\text{eff}}^{\text{lab}}, \theta_{\text{eff}}^{\text{c.m.}})$ is the NN t-matrix connecting the incident and the final channels, and $\gamma = A/(A+1)$ with A being the target mass number. The meanings of the other parameters and suffices are the same as those in Eq. (5).

For consistency with the relativistic calculations, we adopt similar input as far as possible for both models. The distorted waves are solutions to the Schrödinger scattering equation with Schrödinger-equivalent potentials [55] generated from the

same relativistic global potentials employed in the relativistic calculations described above. As for the bound state wave function, we employ the upper component of the relativistic bound state wave function $\Phi_{LJM_j}(\vec{r})$. The t -matrix used is again that deduced from the SP07 phase-shift solution.

In addition to conventional nonrelativistic calculations based on the equation above, calculations with an effective-nucleon-mass correction, where a relativistic dynamical effect is taken into account within the nonrelativistic framework, are performed following a procedure similar to that proposed by Horowitz and Iqbal [56]. For this calculation, the relativistic transition amplitude (5) is expressed in a Schrödinger-equivalent form (SE) as

$$\begin{aligned} T_{LJM_j}^{\text{SE}}(s_a, s_c, s_d) &= \int d\vec{r} [\psi_c^{*(-)}(\vec{r}, \vec{k}_{cB}, s_c) \otimes \psi_d^{*(-)}(\vec{r}, \vec{k}_{dB}, s_d)] \\ &\times \langle \bar{U}_c \bar{U}_d | \hat{F}_{NN}(T_{\text{eff}}^{\text{lab}}, \theta_{\text{eff}}^{\text{c.m.}}) | U_a U_b \rangle [\psi_0^{(+)}(\gamma \vec{r}, \vec{k}_{aA}, s_a) \\ &\otimes \varphi_{LJM_j}(\vec{r})], \end{aligned} \quad (9)$$

whereby the four component wave functions, Ψ_i ($i = a, c, d$) and Φ in Eq. (5), have been approximated by $U_i \psi_i$ and $U_b \varphi$, respectively: ψ_i and φ are the two-component nonrelativistic wave functions in Eq. (8), and U_i is given by

$$U_i(M^*) = \left(\frac{I}{\frac{\vec{\sigma} \cdot \vec{k}}{E^* + M^*}} \right),$$

where $\vec{\sigma}$ denotes the usual Pauli matrices, and I is a 2×2 unit matrix. The momentum operator in the lower component has been approximated by the relevant asymptotic value, \vec{k} , $E^* = \sqrt{k^2 + M^{*2}}$, and M^* is the reduced effective mass of a proton caused by an attractive relativistic scalar potential. Then the quantity $\langle \bar{U}_c(M^* = M) \bar{U}_d(M^* = M) | \hat{F} | U_b(M^* = M) U_a(M^* = M) \rangle$, with nucleon mass M in free space, is simply related to the free NN t -matrix in the nonrelativistic Schrödinger framework. In this way one can incorporate relativistic M^* corrections to the NN scattering matrix. Note that \hat{F}_{NN} refers to the relativistic NN scattering matrix excluding medium corrections. Hence, the inclusion of the nucleon effective mass is taken into account via U_i , while \hat{F}_{NN} is assumed to be independent of the nuclear density.

All of calculations based on the nonrelativistic framework described above are performed using the code THREEDEE [48]. Note that, even though this code is based on the Schrödinger equation, the kinematics are taken to be relativistic.

IV. RESULTS AND DISCUSSIONS

We now compare our relativistic and nonrelativistic predictions to experimental data. In Fig. 3, the measured data presented in Table I are plotted as functions of the effective mean density $\bar{\rho}$ —estimated using the procedure described in Ref. [17]—probed by the knockout reactions from selected s -orbitals in various nuclei. The values of $\bar{\rho}$, in units of the nuclear saturation density ρ_0 , are $0.069\rho_0$, $0.216\rho_0$, and $0.311\rho_0$ for knockout from the $2s_{1/2}$ state in ^{40}Ca , and the $1s_{1/2}$ states in ^6Li and ^{12}C , respectively.

First we look at general features of the experimental data and compare these to a prediction based on the nonrelativistic plane-wave impulse approximation (the thin solid lines). As shown in Fig. 3, all the experimental ($p, 2p$) data change monotonically as a function of density. In addition, their magnitudes are more or less suppressed compared to the corresponding p - p scattering data, which can be considered to be a ($p, 2p$) reaction in a zero density and zero binding-energy target. However, the suppressions for most of the D_{ij} data are reasonably well reproduced by the calculation, while those for A_y and P are not. This is a similar feature observed for the inclusive data described in Sec. I. Namely the suppressions of D_{ij} are interpreted to be mostly caused by changes of the two-body kinematics due to finite reaction Q -values. At the same time, such different features amongst A_y , P , and D_{nn} suggest that simple contaminations of spin-independent processes do not explain these data and that some theoretical corrections are required. One of the main aims of this paper is to identify observables which are sensitive to density-dependent corrections to the NN interaction. However, we first need to quantify the influence of the nuclear medium on the scattering and bound state wave functions. Also, we need to understand the roles of nonrelativistic versus relativistic dynamical processes.

We start by studying the effect of the lower components of the relativistic bound state wave function. For this purpose we compare relativistic to nonrelativistic predictions at the plane wave level, denoted by the thick and thin solid curves in Fig. 3, respectively. Note that owing to the construction of the IA1 representation, the replacement of relativistic scattering and bound state wave functions with positive-energy Dirac plane waves, yields the same values of the free NN transition matrix elements as the corresponding nonrelativistic plane wave matrix elements. Hence, any differences between the relativistic and nonrelativistic plane wave models are attributed to the contribution of the lower components of the four-component relativistic bound state wave function, which are absent in the nonrelativistic two-component wave functions. For the nonrelativistic predictions we employ the upper component radial wave functions of the relativistic bound state wave function as described in the previous section. In general, most observables for the nuclei of interest, with the exception of P , are sensitive to different dynamical treatments of the bound state wave function, thus stressing the important role played by the lower component wave functions inherent to Dirac relativity.

Next we study the effect of distorting optical potentials on the scattering wave functions by comparing both relativistic and nonrelativistic distorted wave predictions to the corresponding plane wave predictions. The nonrelativistic distorted wave results are indicated by thin dashed lines, whereas the relativistic distorted wave predictions are denoted by thick dashed lines in Fig. 3. For the zero recoil kinematics of interest, we observe that nonrelativistic distortion effects are negligible for all polarization transfer coefficients, i.e., the thin solid and dashed lines are essentially the same. On the other hand, by comparing the thick solid and dashed lines, we see that $D_{s's}$ and D_{ll} are sensitive to relativistic distortion effects. The large effect of relativistic distortion is associated with

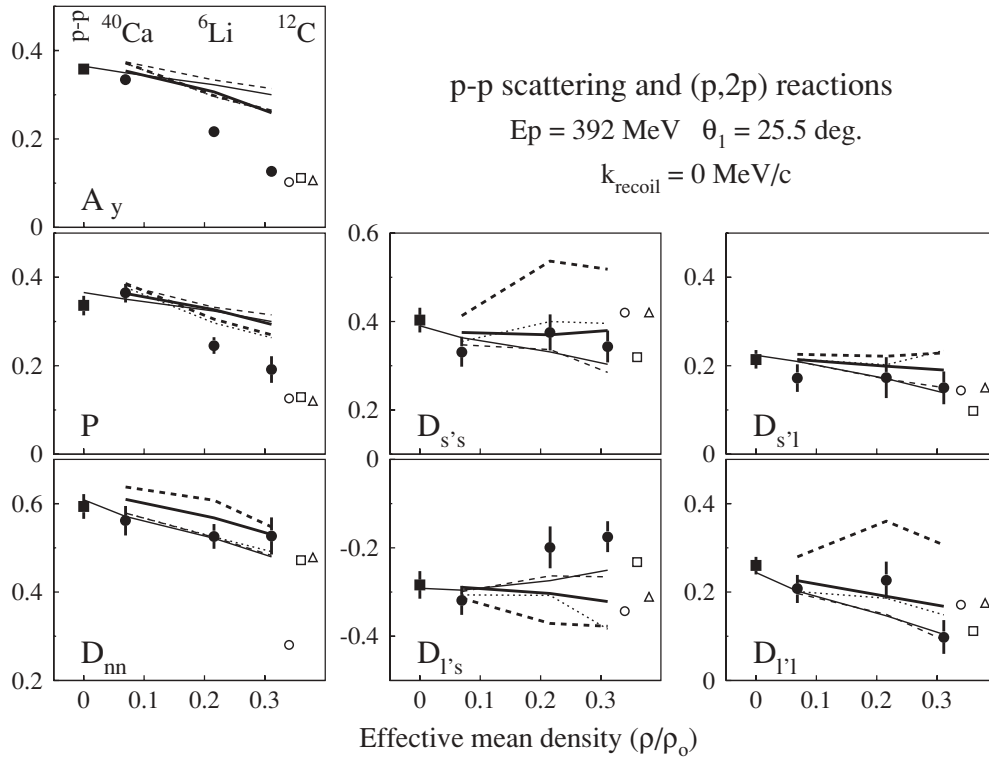


FIG. 3. Comparison of theoretical predictions to experimental data for polarization transfer coefficients, D_{nn} , $D_{s's}$, $D_{s'l}$, $D_{l's}$, $D_{l'l}$, analyzing powers, A_y , and induced polarizations, P , for exclusive proton knockout from the $1s_{1/2}$ states in ${}^6\text{Li}$ and ${}^{12}\text{C}$ as well as from the $2s_{1/2}$ state in ${}^{40}\text{Ca}$ at an incident energy of 392 MeV and for kinematics corresponding to zero recoil momentum as specified in Table I. The data, shown by closed circles, are plotted as functions of the effective mean density (in units of the nuclear saturation density, ρ_0). The closed squares denote the data for p - p scattering. The thin dashed and solid lines respectively denote the nonrelativistic distorted wave and plane predictions, whereas the thick dashed and solid lines respectively represent the relativistic distorted wave and plane wave results. The thin solid lines are connected to p - p scattering points, which are given by the SP07 phase shift solution. The dotted lines represent the nonrelativistic DWIA including relativistic M^* corrections (see text). For $1s_{1/2}$ knockout from ${}^{12}\text{C}$, the open circles correspond to Rho-Brown corrections to the relativistic distorted wave model for $\xi = \chi = 0.85$, whereas the open squares denote the relativistic distorted wave results with modified meson-nucleon coupling constants. The open triangles show results when only the g_σ value is reduced by 4% from parameters used in the calculation denoted by the open squares.

contributions of the lower components of the four-component relativistic scattering wave functions. Note that both relativistic and nonrelativistic distorted wave models fail to consistently describe all polarization data, the most serious discrepancy being for $1s_{1/2}$ knockout from ${}^{12}\text{C}$. This failure is most likely attributed to the exclusion of density-dependent corrections to the NN interaction in both relativistic and nonrelativistic models. Indeed, as already indicated, the effective mean densities for $1s_{1/2}$ knockout from ${}^{12}\text{C}$ is estimated to be about 30% of the saturation density, ρ_0 . Consequently, we expect density-dependent corrections to invoke the largest observable effect for ${}^{12}\text{C}$, which we now consider.

Regarding density dependent corrections, we first study relativistic effective mass M^* type corrections to the nonrelativistic distorted wave model. Essentially this correction provides a crude estimate for the inclusion of the lower components of the relativistic four-component scattering and bound state wave functions which are neglected in conventional nonrelativistic models. Previously [20,25] we demonstrated that M^* corrections to the nonrelativistic distorted wave model reproduce the relativistic distorted wave analyzing power and

induced polarization results for $1s_{1/2}$ knockout from ${}^{12}\text{C}$ at 392 MeV and 1 GeV. The question arises as to whether this correction can consistently reproduce the relativistic distorted wave results for all polarization transfer coefficients. By varying the values of M^* between $0.5M$ and $1.0M$, with M being the free nucleon mass, we establish that M^* values of $0.995M$, $0.965M$ and $0.925M$ reproduce the relativistic distorted wave analyzing powers for ${}^{40}\text{Ca}$, ${}^6\text{Li}$, and ${}^{12}\text{C}$, respectively: the M^* -corrected values are indicated by dotted lines. Keeping these values of M^* fixed we now compare the corrected values to the full relativistic distorted wave results (the thick dashed lines) for all other polarization transfer coefficients. The effect of the M^* correction is to consistently move the nonrelativistic predictions closer to the full relativistic distorted wave results. Note that D_{nn} is insensitive to M^* corrections. With the exception of the analyzing power, however, these corrections fail to describe the relativistic distorted wave results quantitatively. Indeed, there exists no value of M^* which can consistently describe all polarization transfer coefficients. From the preceding analysis we conclude that, with the exception of D_{nn} , relativistic M^* corrections

affect all polarization transfer coefficients. It is also clear that although the relativistic corrections significantly influence spin observables, these corrections cannot quantitatively reproduce the full relativistic distorted wave results, thus stressing the need to use a full relativistic model for studying the effect of Dirac relativity.

Now we consider the effect of density-dependent corrections to the NN interaction within the framework of the relativistic distorted wave model. For implementing nuclear medium corrections, we use the Rho-Brown scaling conjecture [7] described in Sec. III. Indeed we have already demonstrated that Rho-Brown scaling corrections to certain meson masses and meson-nucleon coupling constants shift the relativistic distorted wave predictions in such a way that both analyzing power and induced polarization data are perfectly described for $1s_{1/2}$ knockout from ^{12}C at 392 MeV and 1 GeV [20]. In this paper we study the effect of Rho-Brown scaling corrections to all polarization transfer coefficients. In particular, we only consider $1s_{1/2}$ knockout from ^{12}C since this is where nuclear medium effects are expected to play the most significant role. Furthermore, since there is no definitive prescription for changing coupling constants in the nuclear medium, we adopt the procedure of Krein *et al.* described above, whereby $\xi = \chi < 1$. There is no fundamental reason for choosing $\xi = \chi < 1$, and one could in principle choose values larger than unity. For example, Banerjee [8] claims that g_σ and g_ω increase in the nuclear medium. For consistency with our previous work [20], we choose a Rho-Brown correction factor of $\xi = \chi = 0.850$, the results of which are indicated by open circles in Fig. 3. By construction this value quantitatively describes the analyzing power data, but fails to describe all the polarization transfer coefficients. In particular, it grossly underestimates D_{nn} . The general effect of this correction is to move the distorted wave predictions toward (and sometimes overshooting) the relativistic plane wave results.

One cannot find a value of $\xi = \chi < 1$ which quantitatively describes all the data. Rather than attempting to fully explore the consequences of implementing different combinations of $\xi \neq \chi$, where these values could be less than or greater than 1, in this paper we investigate whether or not it is possible to reproduce all polarization transfer coefficients by slightly changing the values of the coupling constants in the relativistic Horowitz-Love-Franey model [53]. The main purpose of this exercise is to see whether or not it is possible to describe polarization data by only changing the NN interaction parameters. The polarization transfer coefficients are most sensitive to changes in the g_σ and g_ω couplings. We changed the latter couplings by less than 5% and then fine-tuned the other parameters to fit the polarization transfer coefficients for $1s_{1/2}$ knockout from ^{12}C . The correction factors by which the meson-nucleon couplings were multiplied are indicated in brackets next to the relevant couplings, where we use the notation of Ref. [53]: g_σ (1.04), g_ω (0.955), g_δ (0.85), g_π (0.85), g_ρ (1.15), g_{a_0} (0.85), g_{t_1} (0.85), g_{a_1} (1.00), g_{t_0} (1.15), and g_η (1.40). The corrected spin observables are indicated by the open squares in Fig. 3. Note that one should not read too much into the exact values of the meson-nucleon couplings in the nuclear medium, and whether or not these values are less than or greater than 1. The main point is that

one needs to implement corrections at the level of the NN amplitudes in order to provide a good description of the data and, at the same time, spin observables give severe restrictions to these corrections. Actually, each parameter of the NN amplitude affects spin observables differently. The triangles in the figure show a result when only the g_σ value is decreased by 4% from the value used in the calculation denoted by open squares, while other parameters are kept the same. It is found that $D_{s's}$, $D_{l's}$, $D_{s'l}$, and $D_{l'l}$ are significantly shifted, from the open squares, but almost no effect is seen for D_{nn} . The present data present an especially strict test to the relative values of the parameters, including a test for the Rho-Brown scaling conjecture in nuclear field.

V. SUMMARY AND CONCLUSIONS

A complete set of Wolfenstein parameters, D_{nn} , $D_{s's}$, $D_{l'l}$, $D_{l's}$, and $D_{l'l}$, as well as the analyzing powers, A_y , and the induced polarizations, P , have been measured for nucleon knockout reactions, (p , $2p$) reactions, from the $2s_{1/2}$ orbit in ^{40}Ca and the $1s_{1/2}$ orbits in ^6Li and ^{12}C at an incident energy of 392 MeV. We employ a zero recoil kinematical condition, which corresponds to knockout of bound protons with zero momentum in the plane wave limit, where the bound state wave function of the $s_{1/2}$ state is a maximum. It is already known in previous work that A_y and P are significantly reduced from those for free p - p scattering and theoretical predictions based on the NN interaction in free space. In the present study, we observe for the first time that all of $D_{i'j}$ are also more or less reduced from corresponding p - p data. Comparison with nonrelativistic PWIA and DWIA calculations shows that the reduction of $D_{i'j}$, excluding A_y and P , is likely caused by a kinematical effect, namely changes of the two-body kinematics associated with finite Q -values of the (p , $2p$) reactions.

The data are also compared with calculations based on the relativistic DWIA and PWIA models, as well as the nonrelativistic DWIA with a relativistic correction associated with an effective nucleon mass. In these calculations, some nuclear medium effect is included as modifications of the Dirac spinor of nucleons, but the NN scattering matrix is still the same as for scattering in free space. All of these calculations partly explain the A_y reduction as a function of the effective density, but they deviate significantly from the experimental data for most of the $D_{i'j}$. Next, we modified the NN interaction, in the relativistic distorted wave model, via the inclusion of nuclear medium-modified meson masses and coupling constants within the framework of a meson-exchange model, and find a parameter set which reproduces all the experimental data. Even though the resultant parameter set is not necessarily the unique one, the present study shows that these $D_{i'j}$ data give a stringent test to theoretical models of the NN interaction in the nuclear field.

ACKNOWLEDGMENTS

G.C.H. acknowledges support from the South African National Research Foundation under grant no. 2054166 as well as the Japan Society for the Promotion of Science under ID no. L-05525.

- [1] B. D. Serot and J. D. Walecka, in *Advances in Nuclear Physics*, edited by J. W. Negele and E. Vogt (Plenum Press, New York, 1986), Vol. 16, p. 1.
- [2] C. J. Horowitz and B. D. Serot, *Nucl. Phys.* **A368**, 503 (1981).
- [3] For a review, see T. Hatsuda, *Nucl. Phys.* **A544**, 27c (1992).
- [4] V. Bernard, Ulf-G. Meissner, and I. Zahad, *Phys. Rev. Lett.* **59**, 966 (1987).
- [5] B. A. Campbell, John Ellis, and K. A. Olive, *Phys. Lett.* **B235**, 325 (1990); *Nucl. Phys.* **B345**, 57 (1990).
- [6] J. A. McGovern, M. C. Birse, and D. Spanos, *J. Phys. G* **16**, 1561 (1990).
- [7] G. E. Brown and M. Rho, *Phys. Rev. Lett.* **66**, 2720 (1991).
- [8] M. K. Banerjee, *Phys. Rev. C* **45**, 1359 (1992).
- [9] K. Kusaka and W. Weise, *Phys. Lett.* **B288**, 6 (1992).
- [10] T. Hatsuda and S. H. Lee, *Phys. Rev. C* **46**, R34 (1992).
- [11] R. Brockmann and H. Toki, *Phys. Rev. Lett.* **68**, 3408 (1992).
- [12] R. J. Furnstahl, D. K. Griegel, and T. D. Cohen, *Phys. Rev. C* **46**, 1507 (1992).
- [13] S. Gao, R-K Su, and P. K. N. Yu, *Phys. Rev. C* **49**, 40 (1994).
- [14] G. E. Brown, A. Sethi, and N. M. Hintz, *Phys. Rev. C* **44**, 2653 (1991).
- [15] T. Noro *et al.*, *Nucl. Phys.* **A629**, 324c (1998).
- [16] A. A. Cowley *et al.*, *Phys. Rev. C* **57**, 3185 (1998).
- [17] K. Hatanaka *et al.*, *Phys. Rev. Lett.* **78**, 1014 (1997).
- [18] C. A. Miller *et al.*, in *Proceedings of the 7th International Conference on Polarization Phenomena in Nuclear Physics*, Paris, 1990 (Editions de Physique, Les Ulis, France, 1990), p. C6-595.
- [19] C. A. Miller *et al.*, *Phys. Rev. C* **57**, 1756 (1998).
- [20] T. Noro *et al.*, *Phys. Rev. C* **72**, 041602(R) (2005).
- [21] O. V. Miklukho *et al.*, *Nucl. Phys.* **A683**, 145 (2001).
- [22] V. A. Andreev *et al.*, *Phys. Rev. C* **69**, 024604 (2004).
- [23] O. V. Maxwell and E. D. Cooper, *Nucl. Phys.* **A574**, 819 (1994).
- [24] T. Noro *et al.*, *Nucl. Phys.* **A663-664**, 517c (2000).
- [25] G. C. Hillhouse and T. Noro, *Phys. Rev. C* **74**, 064608 (2006).
- [26] T. A. Carey, K. W. Jones, J. B. McClelland, J. M. Moss, L. B. Rees, N. Tanaka, and A. D. Bacher, *Phys. Rev. Lett.* **53**, 144 (1984).
- [27] L. B. Rees *et al.*, *Phys. Rev. C* **34**, 627 (1986).
- [28] C. Glashauser *et al.*, *Phys. Rev. Lett.* **58**, 2404 (1987).
- [29] T. N. Taddeucci *et al.*, *Phys. Rev. Lett.* **73**, 3516 (1994).
- [30] T. Wakasa *et al.*, *Phys. Rev. C* **59**, 3177 (1999).
- [31] C. J. Horowitz and D. P. Murdock, *Phys. Rev. C* **37**, 2032 (1988).
- [32] C. Chan *et al.*, *Nucl. Phys.* **A510**, 713 (1990).
- [33] S. Dieterich *et al.*, *Phys. Lett.* **B500**, 47 (2001).
- [34] S. Strauch *et al.*, *Phys. Rev. Lett.* **91**, 52301 (2003).
- [35] G. C. Hillhouse, J. Mano, A. A. Cowley, and R. Neveling, *Phys. Rev. C* **67**, 064604 (2003).
- [36] G. C. Hillhouse, J. Mano, S. M. Wyngaardt, B. I. S van der Ventel, T. Noro, and K. Hatanaka, *Phys. Rev. C* **68**, 034608 (2003).
- [37] G. Krein, Th. A. J. Maris, B. B. Rodrigues, and E. A. Veit, *Phys. Rev. C* **51**, 2646 (1995).
- [38] T. Noro, K. Hatanaka, K. Hosono, H. Akimune, H. Sakaguchi, M. Yosoi, T. Tamii, and S. Toyama, RCNP Annual Report 1993, p. 167.
- [39] M. Fujiwara *et al.*, *Nucl. Instrum. Methods Phys. Res. A* **422**, 484 (1999).
- [40] K. Hatanaka, K. Takahisa, H. Tamura, M. Sato, and I. Miura, *Nucl. Instrum. Methods Phys. Res. A* **384**, 575 (1997).
- [41] N. Matsuoka, T. Noro, K. Sagara, S. Morinobu, A. Okihana, and K. Hatanaka, RCNP Annual Report 1991, p. 186.
- [42] M. Yosoi *et al.*, in *Proceedings of the 11th International Symposium on High Energy Spin Physics*, edited by K. J. Heller and S. L. Smith, AIP Conf. Proc. No. 343 (AIP, New York, 1995), p. 157.
- [43] S. E. Darden, in *Proceedings of the 3rd International Symposium on Polarization Phenomena in Nuclear Reactions, Madison, 1970*, edited by H. H. Barschall and W. Haeblerli (The University of Wisconsin Press, Madison, 1971), p. 39.
- [44] G. Waters, I. M. Blair, G. A. Ludgate, N. M. Stewart, C. Amsler, R. C. Brown, D. V. Bugg, J. A. Edgington, C. J. Oram, K. Shakarchi, A. S. Clough, D. Axen, S. Jaccard, and J. Vávra, *Nucl. Instrum. Methods* **153**, 401 (1978).
- [45] Y. Ikebata, *Phys. Rev. C* **52**, 890 (1995).
- [46] O. V. Maxwell and E. D. Cooper, *Nucl. Phys.* **A603**, 441 (1996).
- [47] J. Mano and Y. Kudo, *Prog. Theor. Phys.* **100**, 91 (1998).
- [48] N. S. Chant and P. G. Roos, *Phys. Rev. C* **27**, 1060 (1983).
- [49] E. F. Radish, G. J. Stephenson, Jr., and G. M. Lerner, *Phys. Rev. C* **2**, 1665 (1970).
- [50] C. J. Horowitz, D. P. Murdock, and B. D. Serot, in *Computational Nuclear Physics I*, edited by K. Langanke, J. A. Maruhn, and S. E. Koonin (Springer-Verlag, Berlin, 1991), p. 129.
- [51] E. D. Cooper, S. Hama, B. C. Clark, and R. L. Mercer, *Phys. Rev. C* **47**, 297 (1993).
- [52] R. A. Arndt, I. I. Strakovsky, and R. L. Workman, *Phys. Rev. C* **62**, 034005 (2000).
- [53] C. J. Horowitz, *Phys. Rev. C* **31**, 1340 (1985).
- [54] O. V. Maxwell, *Nucl. Phys.* **A600**, 509 (1996).
- [55] L. G. Arnold and B. C. Clark, *Phys. Lett.* **B84**, 46 (1979).
- [56] C. J. Horowitz and M. J. Iqbal, *Phys. Rev. C* **33**, 2059 (1986).